

Accepted Manuscript

Structural basis for the design and synthesis of selective HDAC inhibitors

Simone Di Micco, Maria Giovanna Chini, Stefania Terracciano, Ines Bruno, Raffaele Riccio, Giuseppe Bifulco

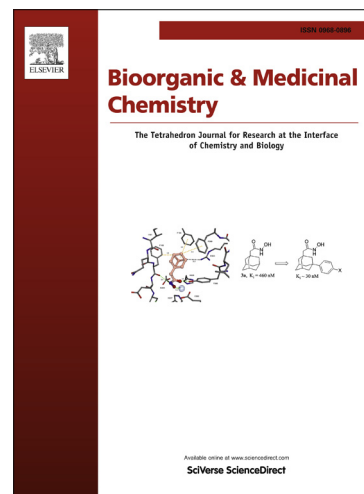
PII: S0968-0896(13)00362-3
DOI: <http://dx.doi.org/10.1016/j.bmc.2013.04.036>
Reference: BMC 10776

To appear in: *Bioorganic & Medicinal Chemistry*

Received Date: 11 January 2013
Revised Date: 9 April 2013
Accepted Date: 10 April 2013

Please cite this article as: Di Micco, S., Chini, M.G., Terracciano, S., Bruno, I., Riccio, R., Bifulco, G., Structural basis for the design and synthesis of selective HDAC inhibitors, *Bioorganic & Medicinal Chemistry* (2013), doi: <http://dx.doi.org/10.1016/j.bmc.2013.04.036>

This is a PDF file of an unedited manuscript that has been accepted for publication. As a service to our customers we are providing this early version of the manuscript. The manuscript will undergo copyediting, typesetting, and review of the resulting proof before it is published in its final form. Please note that during the production process errors may be discovered which could affect the content, and all legal disclaimers that apply to the journal pertain.



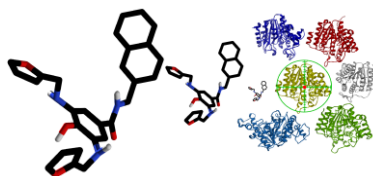
Graphical Abstract

Structural Basis for the design and synthesis of selective HDAC inhibitors

Leave this area blank for abstract info.

Simone Di Micco, Maria Giovanna Chini, Stefania Terracciano, Ines Bruno, Raffaele Riccio, and Giuseppe Bifulco*

Dipartimento di Scienze Farmaceutiche e Biomediche, Università degli Studi di Salerno, Via Ponte Don Melillo, 84084 Fisciano (SA), Italy





Structural basis for the design and synthesis of selective HDAC inhibitors

Simone Di Micco, Maria Giovanna Chini, Stefania Terracciano, Ines Bruno, Raffaele Riccio, and Giuseppe Bifulco*

Dipartimento di Farmacia, Università degli Studi di Salerno, Via Ponte Don Melillo, 84084 Fisciano (SA), Italy

ARTICLE INFO

Article history:

Received

Received in revised form

Accepted

Available online

Keywords:

Antitumor agents

HDAC selective inhibitors

histone deacetylase

molecular modeling

DFT

ABSTRACT

Histone Deacetylases are considered promising targets for cancer epigenetic therapy, and small molecules able to modulate their biological function have recently gained an increasing interest as potential anticancer agents. In spite of their potential application in cancer therapy, most HDAC inhibitors unselectively bind the several HDAC isoforms, giving rise to different side-effects. In this context, we have traced out the structural elements responsible of selective binding for the therapeutically relevant different HDAC isoforms. The structural analysis has been carried out by molecular modeling, docking in the binding pockets of HDAC1-4 and HDAC6-8, thirty six inhibitors presenting a well defined selectivity for the different isoforms. As quick proof of evidence, we have designed, synthesized and experimentally tested three selective ligands. The experimental data suggest that the obtained structural guidelines can be useful tools for the rational design of new potent inhibitors against selected HDAC isoforms.

2009 Elsevier Ltd. All rights reserved.

1. Introduction

Gene expression is highly regulated by post-translational modifications of histone proteins, including acetylation, methylation, phosphorylation, ubiquitylation, sumoylation, ADP-ribosylation, glycosylation, biotinylation and carbonylation.¹ In particular, histone acetyl groups are removed by metalloenzymes called Histone Deacetylases (HDACs).¹ These enzymes, encoded by a family of 18 genes, are grouped into four separate classes.¹ Class I includes HDAC1-3 and HDAC8, which are localized in the nucleus, while class II HDACs, subdivided in Class IIA and Class IIB, is formed by member proteins shuttling between the nucleus and in the cytoplasm. Class IIA includes HDAC4, HDAC5, HDAC7, and HDAC9, and Class IIB comprises HDAC6 and HDAC10. The third class of HDACs are the human sirtuins (SIRT), that are NAD⁺ dependent enzymes.² There are seven human SIRT proteins (SIRT1-7) whose cellular localization include various organelles depending on the function of each protein.³ Class IV only comprises HDAC11, located in the nucleus.

It has been observed that overexpression of HDACs is correlated to cancerous pathologies,⁴ and the different isoforms of HDAC are expressed in several tumor tissues with specific biological function (Table 1).⁵

Please, insert Table 1

Since the increased activity of HDACs is associated with carcinogenesis and tumor progression, HDAC inhibitors have been attracting the attention of the researchers as promising anticancer agents.^{5,6} Several bioactive small molecules of natural or synthetic origin, have been investigated as HDAC inhibitors,^{7,8} and the suberoylanilide hydroxamic acid (SAHA)⁹ and FK228 (Istodax)¹⁰ has been approved by the Food and Drug Administration for the treatment of cutaneous T cell lymphoma.^{9,10} Besides SAHA, other inhibitors have also demonstrated a therapeutic potential use. Most of the currently HDAC inhibitors, tested in clinical trials, are rather unselective, inhibiting either all or at least several members of the HDAC family. Clinical studies show that pan-HDAC inhibitors may give rise to numerous side effects:^{5,10} bone marrow depression, diarrhoea, weight loss, taste disturbances, electrolyte changes, disordered clotting, fatigue, and cardiac arrhythmias. However, the toxicity profile is different for the various pan-HDAC inhibitors, giving rise to different and controversial opinions of their use in cancer therapy. Moreover, the very efficient antitumour effect of HDAC inhibitor should be attributed to the simultaneous inhibition of the different isoforms by blocking different functions of cancer cells. These undesirable effects could be ascribed to the important role of HDACs to regulate different proteins involved in diverse biological processes.⁵ For this reason, selective HDAC ligands may be preferred to pan inhibitors in therapeutic applications.¹² Thus, the next step in the development of HDAC inhibitors is to target selectively

*Corresponding author. Tel.: +39 089969741; fax: +39 089969602.
E-mail address: bifulco@unisa.it (G. Bifulco).

individual HDAC isoforms, with the aim of interfering with critical oncogenic function in cancer cells and without affecting normal cells. It should be also verified if selective inhibitors maintain the efficacy of pan inhibitors and present reduced side effects. In this context, as the enzymes work in cells with other protein partners, it is difficult to devise small molecules able to selectively bind HDACs.¹³ Indeed, HDACs are the catalytic centre of multiprotein clusters.¹³ In literature, studies devoted to develop selective ligands for specific isoforms are reported, even though such studies only consider a restricted number of isoforms.¹⁴ Moreover, most of the published works focused on selective ligands are only based on biological profiles, lacking the structural investigation aimed to disclose the ligand and protein elements potentially responsible of class and isoform selectivity.¹⁵

On this basis, in the present contribution, we have traced out the structural elements responsible of selective binding in the whole landscape of the therapeutically relevant HDAC isoforms (Scheme 1).

Please, insert Scheme 1

In particular, we have tried to rationalize a number of experimental observations and tried to systematically add new structural insights for a targeted design of selective inhibitors of the different HDAC isoforms, focusing our attention on HDAC1-4, and HDAC6-8. HDAC9-11, for which few information so far are available in literature on expression and function in tumor cells, and HDAC5, missing a concrete ligand inhibitory profile,⁵ have not been considered in our investigation.

Our structural analysis was performed by molecular docking calculations, using as ligands pan and class selective HDAC inhibitors reported in the literature (**1-36**, Scheme 2), presenting a well defined profile of HDACs inhibition. Based on the obtained structural guidelines, we designed (**37-39**, Scheme 2), synthesized and experimentally tested selective molecular probes.

Please, insert Scheme 2

2. Methods

2.1. Homology modeling

The amino acid sequences of Human HDAC1 (Genbank Accession Number Q13547,482aa), HDAC2 (Genbank Accession Number AAH-31055,488aa), HDAC4 (Genbank Accession Number BAA22957,1097aa), and HDAC6 (Genbank Accession Number Q6NT75,1215aa), were extracted from the NCBI protein sequence database. The BLAST (Basic Local Alignment Search Tool)¹⁶ search was performed to find homologous proteins in the PDB database, applying the BLOSUM62¹⁷ (BLOCKS of amino acid SUBstitution Matrix) matrix. The search of homologous proteins was run by the Chimera 1.5.3 package.¹⁸ The resulting alignments were examined and modified manually. HDAC1 has additional segment in his C-terminal domain that is about 50-110 amino acids long. When this portion of the sequence was subjected to a BLAST search, no alignment was possible, and no similar sequences (other than itself) were found. Moreover, the function of these residues was proposed to recruit other enzymes to large protein complexes that may regulate their activities.^{19,20} Thus, it may have less influence on the substrate/inhibitor binding. Due to the lack of structural information on this portion, it was omitted in the model building. The three-dimensional structure of HDAC2 chain A (PDB code: 3MAX)²¹ and HDAC4 (PDB code: 2VQM)²² were respectively used as templates for human HDAC1

and HDAC6 homology models building. HDAC6 differs from other HDACs, for the presence of two catalytic domains (HDAC6 CD I and HDCA6 CD II) sharing 46% sequence identity and 60% similarity. In general, CD1 and CD2 show the same relevant amino acid residues in the active site, whereas more differences can be observed in the loop regions. A recent study, using natural and synthetic substrates, showed that the second catalytic site is the major functional domain of HDAC6.²³ In particular, the authors demonstrated that the inhibition of HDAC6 can be solely ascribed to the interaction of ligands with the second binding domain. Moreover, recently, docking studies on HDAC6 have been performed using the second catalytic domain of HDAC6.²⁴ The resulting alignments were used as input for the automated homology modeling program MODELER.²⁵ The number of generated loops was set to five along with high optimization level for models and loops. The generated models of HDAC1 and HDAC6, showing the lowest energy and minor number of restraint violations, were selected. On the obtained homology models, hydrogen atoms were added by using the graphical interface Maestro version 6.0, Schrödinger, LLC, New York, NY, 2003. The charges of side chains were assigned considering their pK_a at physiological pH of 7.4. In particular, Arg and Lys were positively charged, whereas Asp and Glu were negatively charged. The His were neutral. The geometry of the added hydrogen atoms by OPLS force field [26] and steepest descent method (500 steps and convergence threshold 0.5 kJ mol⁻¹ Å⁻¹) by using the MacroModel 8.5.²⁷ The quality of the obtained models for HDAC1 and HDAC6 (see supplementary information) were validated using the software PROCHECK.²⁸

2.2. Quantum mechanical calculations

In order to have an accurate weight of the electrostatics, we derived the partial charge of Zn²⁺ and of the amino acids constituting the catalytic center (Table S2-S9) by DFT calculations m05²⁹ level by the 6-31+G(d) basis set and ChelpG method³⁰ for population analysis (Gaussian 03 Software Package).³¹ By using the same theoretical level, the partial charges of **37-39** were achieved (TableS10-S12). All the partial charges derived from DFT theoretical level were used in the subsequent docking calculations.

2.3. Ligands preparation

All ligands structures were built using the graphical interface Maestro version 6.0, Schrödinger, LLC, New York, NY, 2003, and their geometries optimized through MacroModel 8.5 and using the MMFFs force field.³² For the **36**, the tertiary amine on the tricyclic ring system was protonated and the two enantiomers were considered in our theoretical studies. Monte Carlo Multiple Minimum (MCMM) method (10000 steps) of the MacroModel module was used in order to allow a full exploration of the conformational space. The so obtained geometries were optimized using the Polak-Ribier conjugate gradient algorithm (maximum derivative less than 0.001 kcal/mol). A GB/SA (generalized Born/surface area) solvent treatment³³ was used, mimicking the presence of H₂O in the geometry optimization and in the conformational search steps.

2.4. Molecular docking calculations

Molecular docking studies were performed using AutoDock 3.0.5,³⁴ which has been successfully used in the interpretation of the inhibitory activity of several HDAC ligands.^{19,35,36}

The homology models for HDAC1 and HDAC6 were used in molecular docking calculations, along with the X-ray structures of HDAC2 (3MAX),¹⁹ HDAC3 (4A69),³⁷ HDAC4 (2VQM),²² HDAC7 (3C0Z)³⁸ and HDAC8 (3F0R).³⁹ In particular, the crystal structure of HDAC8 complexed with CRAA-A (1VKG)⁴⁰ was also considered in the calculations, in order to explore the large sub-pocket created by the shift of Phe152 upon ligand binding, and located in the hydrophobic active site channel.

HDACs are metalloproteins, so a non-bonded model for metallic center according to the non-bonded Zn²⁺ parameters of Stote⁴¹ (Zinc Radius = 1.10 Å, well depth = 0.25 kcal/mol) were used in the docking calculations.

To achieve a representative conformational space during the docking studies and taking into account the variable number of active torsions, 10 calculations consisting of 256 runs were performed, obtaining 2560 structures for each ligand (1-39). The Lamarckian genetic algorithm was employed for dockings. An initial population of 600 randomly placed individuals was used. The maximum number of energy evaluations and of generations was set up at 5 x 10⁶ and 6 x 10⁶, respectively. A mutation rate of 0.02 and a crossover rate of 0.8 were used, and the local search frequency was set up at 0.26. Results differing by less than 2 Å in positional root-mean-square deviation (rmsd) were clustered together and ranked by free energy of binding. For all the docked structures, all bonds were treated as active torsional bonds except the amide bonds. The grid box was sized, by using 0.375 Å between the grid points, and the coordinates of grid center were varied for each protein (see supplementary data for the three-dimensional coordinates of the homology models). In details, in docking calculations with HDAC1 as receptor, a grid box size of 66 x 64 x 72 with a grid centre having the following x, y, and z coordinates respectively: 49.75, 5.0 and 105.0. For HDAC2 it was used a grid box size of 66 x 64 x 68 with the grid center positioned on the following x, y, and z coordinates respectively: 66.265, 31.0 and -3.7. For HDAC3 a grid box size of 68 x 86 x 76 with grid center x, y, and z coordinates at 34.423, 60.188 and 26.892, respectively. For HDAC4 a grid box size of 48 x 64 x 90 presenting a grid center with the following x, y, and z coordinates respectively: 16.376, -10.087 and 2.96. For HDAC6 a grid box size of 54 x 60 x 62 with a grid center positioned on the following x, y, and z coordinates respectively: 18.908, -9.0 and -0.126. For HDAC8 (3F0R) a grid box size of 66 x 66 x 72 was used, and it presented a grid center with the following x, y, and z coordinates respectively: 107.7, 59.3 and 26.383. For HDAC8 (1VKG, pdb ID) the grid box size was 62 x 62 x 62 and the grid center at the following x, y, and z coordinates respectively: 21.859, 69.0 and 72.5.

2.5. Chemistry

2.5.1. General Experimental Procedures

All the NMR spectra (¹H, HMBC, HSQC) were recorded on a Bruker Avance DRX600 at T = 298 K. The compounds (37-39) were dissolved in 0.5 mL of 99.8% d₄-MeOH (Aldrich, 99.8+ Atom % D). Chemical shifts are expressed in parts per million (ppm) on the delta (δ) scale. Electrospray mass spectrometry (ES-MS) was performed on a LCQ DECA TermoQuest (San José, California, USA) mass spectrometer. Analytical and semipreparative reverse phase HPLC was performed on a Jupiter C-18 column (250 x 4.60 mm, 5 μ, 300 Å, flow rate = 1 mL/min; 250 x 10.00 mm, 10 μ, 300 Å, flow rate = 4 mL/min respectively). The binary solvent system (A/B) was as follows:

0.1% TFA in water (A) and 0.1% TFA in acetonitrile (B). The absorbance was detected at 220-240 nm. All the solvents used for the synthesis were HPLC grade; they were purchased from Aldrich, Fluka, Carlo Erba. All reagents were purchased from commercial suppliers and used as received. All the reactives were purchased from Aldrich.

2.5.2. Synthesis of amides: general procedure

The carboxylic acid **40** or **41** (1 equiv.) and the appropriate ammine **42** or **43** (2 equiv.) were dissolved in DMF. *N,N*-triethylamine (TEA), *N*-hydroxybenzotriazole (HOBt) and *N,N'*-diisopropylcarbodiimide (DIC) (2 equiv. of each) were added. The mixture was leaved at room temperature for 48 hours under stirring. When TLC showed the consumption of the carboxylic acids **40** or **41**, the reaction was stopped adding HCl 1N (10 mL). The aqueous phase was extracted with ethyl acetate (3 x 10 mL) and the organic phase was washed firstly with a saturate solution of NaHCO₃ and then with brine. Afterward the organics were dried over Na₂SO₄, filtered and concentrated *in vacuo*. The crude was purified by flash chromatography (10 % ethyl-acetate/*n*-hexane to 50 % ethyl-acetate/*n*-hexane) to obtain the desired amidic derivatives as yellow powder (Yields: 78-82 %).

4-hydroxy-*N*-(naphthalen-2-ylmethyl)-3,5-dinitrobenzamide (**45**): ¹H-NMR δ (600 MHz; CH₃OH) 8.51 (2H, s), 8.11 (d, 1H), 7.86 (d, 1H), 7.78 (d, 1H), 7.51-7.43 (m, 4H), 5.01 (2H, s); ES-MS calcd. for C₁₈H₁₃N₃O₆ 367.1; found *m/z* 368.0 [M+H]⁺.

(4-hydroxy-3,5-dinitrophenyl)(pyrrolidin-1-yl)methanone (**46**): ¹H-NMR δ (600 MHz; CH₃OH) 8.51 (2H, s), 3.62 (4H, m), 2.01 (4H, m); ES-MS calcd. for C₁₁H₁₁N₃O₆ 281.1; found *m/z* 282.2 [M+H]⁺.

N-benzyl-2-(4-hydroxy-3,5-dinitrophenyl)acetamide (**47**): ¹H-NMR δ (600 MHz; CH₃OH) 8.22 (2H, s), 7.28 (5H, m), 3.63 (2H, s); ES-MS calcd. for C₁₅H₁₃N₃O₆ 331.1; found *m/z* 332.0 [M+H]⁺.

2.5.3. Reduction of nitro-derivatives to amines: general procedure

A solution of **45-47** and stannous chloride dihydrate (5 equiv.) in ethanol was stirred at 80 °C for about 30 min. The solvent was removed *in vacuo*. Ethyl-acetate (10 mL) was added to the residue and washed with saturated sodium bicarbonate (2 x 10 mL). The organic layer was dried over Na₂SO₄ and concentrated to obtain yellow solids. The obtained compounds **48-50** were directly employed in the next step without further purification.

2.5.4. Reductive amination: general procedure

Under inert atmosphere (N₂), 2 equiv. of aldehyde **51-53** were dissolved in anhydrous CH₃OH (1 mL/0.15 mmol of amine). The mixture was kept under stirring at room temperature; anhydrous amine **42-44** (1 equiv.), ZnCl₂ (1 equiv.) and NaCNBH₃ (2 equiv.) were added. After 1.5 h, when the amine disappeared, the reaction was stopped and 10 mL of an aqueous solution of NaOH 0.1 M was added. After concentration of CH₃OH *in vacuo*, the aqueous phase was extracted with ethyl acetate (3 x 10 mL) and the organics were dried over Na₂SO₄, filtered and concentrated *in vacuo*. The obtained oil was purified on semipreparative RP-HPLC (5% acetonitrile to 100% acetonitrile) to obtain the desired products as yellow powder with a purity > 98 %.

3,5-Bis-[(furan-2-ylmethyl)-amino]-4-hydroxy-N-naphthalen-2-ylmethyl-benzamide (**37**): RP-HPLC: from 10% B to 80% B over 55 min: $t_R = 31.67$ min.; Yield: 49%; $^1\text{H-NMR } \delta$ (600 MHz; CH_3OH): 8.11 (2H, d), 7.91 (2H, d), 7.85 (2H, d), 7.58-7.45 (8H, m), 7.16 (1H, s), 5.02-4.97 (6H, m); $^{13}\text{C-NMR } \delta$ (150 MHz; CH_3OH): 172.7, 129.4, 128.9, 127.1-125.1, 124.1, 117.6, 43.0-42.6. ES-MS calcd. for $\text{C}_{28}\text{H}_{25}\text{N}_3\text{O}_4$: 467.18; found 468.0 $[\text{M}+\text{H}]^+$.

{4-Hydroxy-3,5-bis-[(thiazol-2-ylmethyl)-amino]-phenyl}-pyrrolidin-1-yl-methanone (**38**): RP-HPLC: from 10% B to 50% B over 50 min: $t_R = 18.15$ min.; Yield: 46%; $^1\text{H-NMR } \delta$ (600 MHz; CH_3OH): 7.79-7.66 (4H, br s), 7.50 (2H, br s), 4.66 (4H, s), 3.50 (1H, m), 3.42 (1H, m), 3.21 (1H, m), 3.08 (1H, m), 1.92 (1H, m), 1.86 (1H, m), 1.81 (1H, m), 1.73 (1H, m); $^{13}\text{C-NMR } \delta$ (150 MHz; CH_3OH): 174.5, 142.7-141.0, 120.4-119.0, 50.9, 50.8, 47.5, 47.3, 27.5, 27.13, 27.0, 26.9. ES-MS calcd. for $\text{C}_{19}\text{H}_{21}\text{N}_5\text{O}_2\text{S}_2$: 415.11; found 416.1 $[\text{M}+\text{H}]^+$.

N-benzyl-2-(4-hydroxy-3,5-bis((thiophen-2-ylmethyl)amino)phenyl)acetamide (**39**): RP-HPLC: from 10% B to 60% B over 45 min: $t_R = 30.96$ min.; Yield: 47%; $^1\text{H-NMR } \delta$ (600 MHz; CH_3OH): 7.27 (2H, m), 7.22-7.17 (5H, m), 6.88-6.81 (5H, m), 6.75 (1H, s), 4.39 (4H, s), 4.33 (2H, s), 3.36 (2H, s); $^{13}\text{C-NMR } \delta$ (150 MHz; CH_3OH): 172.0, 129.2-126.0, 127.4-127.1, 44.3, 44.1. ES-MS calcd. for $\text{C}_{25}\text{H}_{25}\text{N}_3\text{O}_2\text{S}_2$: 463.14; found 464.1 $[\text{M}+\text{H}]^+$.

2.6. Biological assay

The screening was performed by Reaction Biology Corp. (www.reactionbiology.com/). Compounds **37-39** were tested in 10-dose mode with 3-fold serial dilution starting at 100 μM in DMSO. TSA (reference compound) was tested in a 10-dose with 3-fold serial dilution starting at 10 μM , and starting at 20 μM with Class2A substrate. In the screening, HDAC1, HDAC2, HDAC4 and HDAC6-8 were used as isolated recombinant human protein; whereas HDAC3 was used as HDAC3/NcoR2 complex. The substrate for HDAC1-3, and HDAC6 was the fluorogenic acetylated peptide based on residues 379-382 of p53 (Arg-His-Lys-Lys(Ac)). For HDAC8, the substrate was the diacetylated peptide based on residues 379-382 of p53 (Arg-His-Lys(Ac)-Lys(Ac)). For HDAC4 and HDAC7, the substrate was Acetyl-Lys(trifluoroacetyl)-AMC. The Reaction Buffer was: 50 mM Tris-HCl, pH 8.0, 137 mM NaCl, 2.7 mM KCl, 1 mM MgCl_2 , 1 mg/ml BSA. The assay conditions were as follow.

HDAC1: 75 nM of HDAC1 and 50 μM of substrate were in the reaction buffer and 1% of DMSO final concentration of tested compounds. Incubation for 2 hours at 30°C.

HDAC2: 5 nM of HDAC2 and 50 μM of substrate were in the reaction buffer and 1% of DMSO final concentration of tested compounds. Incubation for 2 hours at 30°C.

HDAC3: 2.3 nM of HDAC3 and 50 μM of substrate were in the reaction buffer and 1% of DMSO final concentration of tested compounds. Incubation for 2 hours at 30°C.

HDAC4: 665 nM of HDAC4 and 50 μM of substrate were in the reaction buffer and 1% of DMSO final concentration of tested compounds. Incubation for 2 hours at 30°C.

HDAC6: 12.6 nM of HDAC6 and 50 μM of substrate are in the reaction buffer and 1% of DMSO final concentration of tested compounds. Incubation for 2 hours at 30°C.

HDAC7: 962 nM of HDAC7 and 50 μM of substrate are in the reaction buffer and 1% of DMSO final concentration of tested compounds. Incubation for 2 hours at 30°C.

HDAC8: 119 nM of HDAC8 and 50 μM of substrate are in the reaction buffer and 1% of DMSO final concentration of tested compounds. Incubation for 2 hours at 30°C.

3. Results and Discussion

3.1. Structural analysis.

All the considered compounds in the present contribution were analyzed by molecular docking calculations on HDAC1-4 and HDAC6-8 (Scheme 2). We refined some enzyme calculation parameters related to the electrostatic and Van der Waals terms of binding energy, following the successful strategy adopted for the structural studies on azumamide E and two stereochemical variants.³⁵ This strategy allowed to reach a good qualitative accordance between theoretical K_D and biological assays results, and it was also validated by its useful application to the study of other HDAC ligands.³⁶ In particular, for the electrostatic contribution, the partial charges of the zinc ion and the amino acids constituting the catalytic site of each isoforms were calculated at DFT/M05²⁹ theory level by using the 6-31+g(d) as basis set and the ChelpG method³⁰ for the population analysis and were used in the subsequent docking calculations. Similarly, for the van der Waals term the well depth and zinc radius proposed by Stote and Karplus were applied.⁴¹

3.2. Common structural features of all isoforms

As well defined by previous studies,^{7,8} the general structure of HDAC inhibitors can be dissected (**1**, Scheme 2) in: a cap group involved in the molecular recognition process with surface amino acids; a linker, usually hydrophobic; a zinc-chelating group. Each structural moiety contributes to the binding event and biological activity of the small molecules. In particular, a fundamental structural element to inhibit these biological targets is the metal binder. Many chelating agents, such as hydroxamic acids, carboxylate, α -hydroxy-ketone were introduced, and theoretical and experimental evidence showed their ability to coordinate the prosthetic group of the investigated enzymes. Class I and II proteins present a considerable sequence similarity in the catalytic site. By comparing homology and experimental models, we observed the presence of two parallel phenylalanine units delineating the channel which accommodates the acetylated lysine of the histone (Table S1, and Figure S1). As revealed by our docking calculations on all considered HDACs, the switching from a linear carbon chain (TSA (**1**), **3**, **4**, **5**, **23-35**) to an aromatic linker (**2**, **6-22**, **36**) causes an increased affinity with the targets, thanks to favourable π - π interactions with the above mentioned two phenylalanine side chains.

3.3. General features and differences of Class I and Class II

In our analysis we observed that HDAC1-3 and HDAC8 present a CO of a glycine and side chain of a tyrosine pointing inside the 11 Å channel: Gly149 and Tyr303 for HDAC1, Gly154 and Tyr308 for HDAC2, Gly143 and Tyr298 for HDAC3, and Gly151 and Tyr306 for HDAC8. The class I isoform selective compounds **7-16** present an amide bond between the linker and the metal binder (Figure 1). The NH of the amide functionality can establish a hydrogen bond with the carbonyl of the glycine. Moreover, the hydrophobic channel of class II proteins does not display acceptors and donors of hydrogen bonds. In this perspective, the linker could be modified

inserting hydrogen bond acceptors and donors in order to give interactions with these two residues constituting the hydrophobic channel, sustaining selectivity for class I HDACs.

Please, insert Figure 1

The analysis of crystal structures of bacterial homologues (HDLP) of class I⁴² along with human HDAC2,²¹ HDAC3³⁷ and HDAC8³⁹ reveals the presence of a 14 Å internal cavity at the bottom of the 11 Å hydrophobic channel, close to the zinc active site.⁴³ The high sequence similarity of HDAC1 with HDLP, HDAC2, HDAC3 and HDAC8 confirm for all class I HDACs the presence of the 14 Å internal cavity is expected. Our homology model of HDAC1 HDAC3 in fact showed the presence of the internal channel observed in HDLP, HDAC2, HDAC3 and HDAC8, also in agreement with previously reported homology modelling studies.¹⁹ With one exception (HDAC8), the residues forming the 14 Å internal cavities are identical across the different proteins of class I. Recently, 2-amino benzamides were proposed as metal binders, and compounds presenting this functionality showed selectivity for class I enzymes.⁴⁴ In particular, in agreement with reported experimental data, the analysis of docking results on the compounds presenting a benzamide as metal binder (**7**,⁴⁵ Scheme 2) revealed a preference for class I enzymes, in particular for HDAC1 and HDAC2. The coordination of the enzyme prosthetic group by the NH₂ of benzamide requires a side accommodation of phenyl ring, unlike the common metal binders, such as hydroxamic acid, carboxylate group, α -hydroxy-ketone. The consequence is the requirement of a side room at the bottom of the 11 Å channel, offered by the 14 Å internal cavity.

In literature it is reported that natural cyclopeptides⁴⁶ are selective inhibitors of class I proteins, and the most important of these ligands were considered in our studies. For example, the azumamide E,³⁵ Fk228¹⁰ and apicidine⁴⁷ (**3-5**, Scheme 2) show selectivity for class I, with significant affinity for HDAC8 and superior affinity for HDAC1-3. From our theoretical analysis of cyclopeptides and the other ligands, we found that the macrocycle can be accommodated on a shallow pocket located on the protein surface at the entrance of 11 Å hydrophobic cavity, establishing Van der Waals interactions and hydrogen bonds (Figure S2). These interactions contribute to the complex stability, favouring the binding for the HDACs of class I over the isoforms of class II. Such observation is suggested from the docking analysis of the binding mode of azumamide E and apicidine with HDACs of class II, showing that the macrocycle does not interact with macromolecular counterparts on the surface of HDAC4, HDAC6 and HDAC7, thus not contributing to the affinity for the protein.

The pan inhibitors TSA (**1**) and NVP-LAQ824 (**2**),⁴⁸ for example, did not present this structural bulky cap group, highlighting the role of the peptidic macrocycle in dictating the selective class I binding. Compared to other analyzed class I selective ligands, the cyclopeptides presented a wider cap group, which established more extended contacts with proteins surface.

3.4. HDAC1

The differences between HDAC1 and HDAC2 are very small due to an 85 % sequence identity and 93 % sequence similarity, which confer very similar shapes for all the protein regions. The comparison of the three-dimensional models of HDAC1 and HDAC2 reveals some small differences, which could be exploited to discriminate the recognition of these two isoforms.

By our investigation we observed a tighter access to the catalytic site of HDAC1 compared to HDAC2 (Figure 2), due to the different spatial arrangement of residues leading to the zinc ion and bordering the 11 Å channel. In particular, this diverse orientation reflects the replacement of Met233, Pro361 and Met364 in HDAC2 by Leu228, Asn356 and Leu359 in HDAC1.

Please, insert Figure 2

As reported above, all proteins of class I present an internal hydrophobic pocket at the bottom of the channel accommodating the substrate. We observed that the amino acids constituting this internal cavity are identical or conservatively substituted, but differences in the surrounding amino acids of these internal cavities can be pointed out. In particular, bulkier residues in HDAC3 and HDAC8 (see below) prevent the accommodation of the chelating agent with an appendage. Indeed, in the case of HDAC1 and HDAC2 the docking results on **7** highlighted that the metal binder is well harboured and the zinc is coordinated by the CO and NH₂ functionalities. Our docking studies show (Figure S3) that the phenyl ring interacts with the surrounding hydrophobic residues and along with the bidentate coordination increases the affinity for HDAC1 and HDAC2. Our findings are in agreement with published biological assays,⁴⁵ which show the selectivity of MS275 (**7**) for HDAC1 with this preference: HDAC1 > HDAC3 and HDAC1 >> HDAC8, confirming the presence of the benzamide metal binder for directing isoform selectivity.^{7,8,44} The insertion of a substituent on the benzamide leads to a further discrimination among HDACs of class I. Indeed, HDAC1 and HDAC2 were able to harbour a substituent on the benzamide (**8-16**, Scheme 2), such as thiophene or phenyl.⁴⁹ Our docked pose (Figure S4) suggests the same considerations for compound **17**⁵⁰ where the phenethyl replaces the benzamide interacting with the internal cavity, and strengthening the coordination of the zinc to the carbonyl group.

3.5. HDAC2

As outlined in the previous section, many structural elements of compounds having high affinity for HDAC1 are similar for the isoform 2. By comparing the models of HDAC1 and HDAC2, a structural differences, even though small, are detectable. As described above, residues bordering the \approx 11 Å channel, present a different spatial arrangement of Tyr204 in HDAC1 with respect to Tyr209 in HDAC2, in turn depending on the presence of Leu228, Asn356 and Leu359 in HDAC1 and Met233, Pro361 and Met364 in HDAC2. On the basis of this different arrangement, a deeper cavity is present for HDAC2 compared to the shallower cavity of isoform 1, formed by amino acids His183, Tyr209, Phe210 and Leu276. Together with this first discrimination, and even though the amino acids constituting the 14 Å internal cavity are identical for HDAC1 and 2, differences could be found in the neighbouring residues. In details, we observed that the Val19 (HDAC1) is substituted by the Ile24 in HDAC2, influencing the arrangement of surrounding residues. In particular, it was observed a different disposition of Met35, Phe114 and Leu144 giving rise to a larger room compared to HDAC1 (Figure 3). This can justify the observed slightly preference (about 10 fold)^{7,50} of benzamides for HDAC1 vs. HDAC2, due to closer contacts with the internal cavity of isoform 1. Moreover, we calculated volume (CASTp server)⁵¹ of catalytic sites of isoforms 1 and 2 observing for HDAC2 414.8 Å³ vs. 281.7 Å³ of HDAC1. The isoforms 2 showed also a wider pocket area of 409.2 Å² vs. 327.7 Å². The opening mouth area is 23.3 Å² for HDAC2 and 12.9 Å² for HDAC1. We designed and tested new potential selective ligand for HDAC2 taking into

account the combination of a metal binder able to interact with the 14 Å internal cavity and of an adapted capping moiety (see below).

Please, insert Figure 3

3.6. HDAC3

As shown in the previous two sections, the relevant structural elements to discriminate isoforms of class I are appendages of metal binder, able to interact with the internal cavity at the bottom of the 11 Å channel. By the analysis of the amino acids surrounding the internal cavity close to the catalytic site, we observed that in HDAC3 Tyr107 replaces Ser113 in HDAC1 and Ser114 in HDAC2. In the isoform 3 the presence of the bulkier side chain of Tyr107, forces the Leu133 to point towards the center of the internal cavity. This shift of Leu133 causes a steric clash preventing the accommodation of bulky metal binders. Our docking results on **8-17** highlighted that the metal binder was not well accommodated in the internal cavity, as experimentally confirmed.^{7,8,45,50} Thus, the design of an adapted chelating agent able to match the HDAC3 macromolecular counterparts and to give effective contacts, is necessary for gaining selectivity toward this isoform.

Our investigation allowed to appreciate differences on the protein surface near the catalytic site. In particular, we observed the presence of Phe199 in HDAC3 and Tyr204 and Tyr209 in HDAC1 and HDAC2, respectively. In the isoforms 1 and 2 the OH group of tyrosine establishes a hydrogen bond with the CO of Leu271 in HDAC1 and Leu276 in HDAC2. This hydrogen bond is absent in HDAC3, giving rise to a shallower hydrophobic cavity delimited by the amino acids Ile171, His172, Phe199, Phe200, Gly267 and Cys268 (Figure S5). The absence of the OH implies no possible hydrogen bonds formation with the ligands. Moreover, HDAC3 differs from all other isoforms for the presence of a solvent-exposed tyrosine (Tyr198) on the surface of the enzyme (Figure 4).

Please, insert Figure 4

This residue is very close to the active site tunnel, changing the shape of the protein surface in that point. In particular, its carbonyl group of the backbone points could be involved with hydrogen bonds with the ligands.

3.7. HDAC8

The resolved X-ray structures of HDAC8 complexed with TSA (**1**)³⁹ and **18**⁵² have suggested structural elements to selectivity bind this isoform. When bound to **18**, HDAC8 shows a shift from the normal position of Phe152, which is located along the hydrophobic 11 Å channel. This shift creates a sub pocket that can contain hydrophobic groups protruding from the linker moiety, extending Van der Waals contacts with the channel of HDAC8. These further strong interactions contribute to the complex stability and favour a selective binding to HDAC8. Compounds **19**^{14b}, **20**^{15b} and **22**⁵³ were designed on the structural considerations obtained from **18** bound to HDAC8, and molecular docking calculations showed, as expected, high selectivity for HDAC8 thanks to the interactions with the induced hydrophobic cavity. By comparing the amino acids constituting the internal cavity found in all isoforms of class I, we observed that HDAC8 presents Trp141, in place of a leucine in HDAC1-3. The presence of the bulky side chain of Trp141 hinders the appropriate accommodation of chelating portions endowed with appendages, compared to HDAC1-3. Indeed, our docking results on **7** with HDAC8 showed that the Trp141 limited the accommodation of the benzamide, causing the NH₂ to coordinate the zinc ion in a monodentate manner (Figure S6). Moreover, for

compounds **8-17** endowed of larger appendages, the prosthetic group of the enzyme is not coordinated. On the other hand, well tailored chelating moieties can afford selectivity for isoform 8, as showed by compounds **23** and **24**.^{14a} Indeed, the N-thiomethylazetidin-2-one contained in **23** and **24** interacts with Trp141, allowing a correct coordination of the zinc binding region of HDAC8 (Figure S7).

3.8. HDAC4

Based on docked poses of all considered ligands (Scheme 2), we tried to trace out the structural elements responsible for the selectivity of HDAC4. In particular, aryl pyrrolyl hydroxamide (APHA, **25**, **26**, Scheme 2) compounds⁵⁴ are reported as selective HDAC4 inhibitors. These compounds show a lower general HDAC affinity compared to TSA, but present higher selectivity for this enzyme. It was observed that substitution of chlorine with fluorine at phenyl C3 position improved the selectivity for HDAC4 from 78-fold to 176-fold over class I.⁵⁴ Moreover, non-halogenated or differently substituted APHA derivatives did not show any selectivity towards this isoform, highlighting the importance of the position of the halogen in the capping group. Our theoretical model showed that the halogen is involved in a hydrogen bond with the side chain of Tyr170 (Figure 5). Moreover, there is an interaction between NH group of Phe168 with the electron π system of the halogenated phenyl ring, along with a π - π interaction of C-halogen bond with CO of Phe168 that can contribute to the specific recognition for HDAC4. Even though the Phe is conserved in the other isoforms, the APHA cap group interacts only with backbone amide of Phe168 of HDAC4 due to different shape of residue at rim of catalytic channel. Our theoretical investigation also suggested that the presence of an aromatic linker in **25** and **26** gives rise to π - π interactions with side chains of Phe168 and Phe227 (Figure 5).

Please, insert Figure 5

Not surprisingly, the hydroxamic acid of **25** and **26** coordinated the zinc ion, but also established hydrogen bonds with the N⁶² of His158 and His159 by the OH and NH groups, respectively (Figure 5).

As reported above,⁵⁴ a moderate biological activity has been shown for these HDAC4 selective inhibitors, thus structural modifications are required to increase the affinity of new candidate molecules. From our analysis, hydrophobic cavity delimited by residues His198, Phe226, Phe227, Leu299 may host a larger group, able to establish a hydrogen bond with the NH of His198, in replacement of the methyl group in the **25** and **26**. From the docked poses of **25** and **26** we observed the cap group near a small pocket formed by Pro165, Met166, Gly167, Tyr170, and Cys169. Thus, along with a halogen, a hydrophobic group can be inserted to establish Van der Waals contacts with the described pocket on protein surface. Our comparison of electrostatic potential maps of all considered isoforms on the surface around the channel leading to the zinc ion revealed that HDAC4 displayed a positive charged area, whereas the other proteins presented negative or neutral regions (Figure S8). Thus, the cap moiety can be elongated to favour electrostatic interactions with side chains of positively charged amino acids.

3.9. HDAC6

As already reported in previous studies on selective HDAC6 ligands,^{14d,14e,15a} we confirmed through our analysis that the linker length is a crucial structural element for achieving selectivity.

Upon zinc coordination, the linker length is responsible of correctly directing the extended interactions of the capping moiety with the macromolecular counterparts. HDAC6 presents a wider entrance of the binding pocket conducting to the prosthetic group, formed by several non-polar residues. The selective inhibitors (**27-35**) of HDAC6 follow the protein shape by their structural moieties and can assume an extended conformation interacting with the non-polar residues on protein surface (Figure S9). In the case of other considered HDAC isoforms, due to the smaller entrance of the hydrophobic channel, the cap groups are not well accommodated in the surface cavities giving fewer contacts with amino acids, and suggesting a consequent lower contribution to the complex stability. Moreover, in our docked poses the linker chain of **27-35** folds to allow contacts between cap group and amino acids on the surface of HDAC1-4, HDAC7 and HDAC8, but this entropic loss is not compensated by extended interactions with the macromolecular counterparts. These theoretical findings agree with experimental observations that all selective inhibitors for HDAC6, tubacin (**27**),⁵⁵ mercaptoacetamides (**28-31**),^{15b} and their analogues (**32-35**)⁵⁶ presented longer spacers, differently from class I selective inhibitors whose optimal linker length is six carbons.^{7,8,35,36} As recently reported (**36**, Scheme 2),⁵⁷ the right combination of linker length with a large and rigid cap group can also dictate the selectivity for the isoform 6. The **36** presents a shorter linker length compared to the other selective HDAC6 compounds (**27-35**), but the tolyl linker combined with the tricycle confers a bent conformation to **36**, favouring tight interactions with the rim of hydrophobic channel of this isoform. On the contrary, the docked poses of **36** in the binding cavity of HDAC1-4, HDAC7 and HDAC8 shows steric clashes with amino acids on the proteins surface, leading to unfavourable ligand-enzyme binding.

3.10. HDAC7

Up to date, there are not selective inhibitors of HDAC7. Thus, the docking results of compounds **1-36**, the structural features of the catalytic domain and of the surface pockets of HDAC7 may suggest interesting elements for designing selective inhibitors of this isoform. In detail, the unique sequence of HDAC7 gives rise to a novel zinc binding motif. This protein domain is formed by a β -hairpin positioned by two antiparallel β -strands (β 3 and β 4) and the loop between helices α 1 and α 2, which outlines a distinct and only groove contiguous to the opening of the active site channel.³⁸ This enlarged active site of HDAC7 could be able to harbour a well tailored metal binder, conferring selectivity and improving the affinity of new inhibitors for this enzyme. Selective inhibitors **8-17** presented a metal binder with an appendage able to interact with the 14 Å internal cavity of class I proteins. Our docking results on HDAC7 showed that these selective inhibitors did not coordinate the prosthetic group of the enzyme and did not fill the enlarged active site due to the steric hindrance. Our predicted bioactive conformation of **7** is bound to the zinc ion in a monodentate fashion. On the contrary, the remainder docked inhibitors, presenting a classical chelating agent without decorative appendages, coordinate the zinc ion. Thus, in the hypothesis to design selective binders of HDAC7, new protuberances decorating the metal binder should be projected to selectively match the active site of HDAC7. It could be suggested to insert two flexible appendages flanking the metal binder of the putative ligand. We observed a deep hydrophobic pocket near the Phe679, which is a constituting residue of hydrophobic channel harbouring the acetylated lysine. This cavity is delimited by the amino acids His531, His541, Pro542, Glu543, Ile628 and Phe679 (Figure S10), and it is a peculiarity of

HDAC7. The docked poses of **1-36** did not show interactions with this macromolecular counterpart by their cap groups. Thus, a capping moiety, able to establish contacts with this unique pocket on the surface, can be another structural element addressing selectivity for this enzyme.

4. Quick proof of concept: Design, synthesis and biological evaluation of selective binders

4.1. Design of 37-39

On the basis of our analysis aimed to find the structural elements responsible for a specific recognition of HDAC isoforms, we designed three molecular probes (**37-39**, Scheme 2) for the selective inhibition of HDACs. In particular, our design relied on the use of the weak carbonyl group as chelating agent in order to emphasize the contribution to selective binding by the other structural moieties. We designed a metal binder with three different appendages in order to probe the influence on the class I and isoform selectivity. As cap group, we introduced three five-membered heterocycles, able to form hydrogen bonds with the protein. Our calculations suggest that all the three heterocycles established hydrogen bonds with the enzymes with comparable contribution to the binding affinities. For this reason, we did not consider all the combination of cap groups and chelating portion, and we focused on the exploration of the chemical diversity of the synthesized compounds.

The three compounds (**37-39**, Scheme 2) were docked on all considered HDACs. As revealed by the theoretical investigation, the metal binder showed a Class I recognition preference. In fact, the structure of the metal binder presents an appendage able to establish contacts with the internal cavity near the catalytic site. Moreover, changing the structure of the decorative element of the metal binder, we observed isoform selectivity as predicted by the investigation of **1-36**. Indeed, compound **37** selectively reached the catalytic site of HDAC2. In all other isoforms, **37** was not able to coordinate the zinc ion, suggesting an exclusive binding to HDAC2 as confirmed by the biological assays (see next section). In particular, the carbonyl moiety coordinates the zinc ion, whereas the NH of the amide group, as suggested by our analysis, establishes hydrogen bonds with the CO of Gly154 (Figure 6). The naphthalene was accommodated in the 14 Å internal cavity, giving hydrophobic interactions with the surrounding protein amino acids: Met35, Phe114, Gly143, Leu144, Gly305, Tyr308 (Figure 6). The aromatic linker interacted by π - π contacts with the hydrophobic channel conducting to the zinc ion. One of the two furans was accommodated in a shallow pocket delimited by residues His183, Tyr209, Phe210 and Leu276, and it also established π - π interactions with Tyr209 (Figure 6) and was hydrogen bonded with His183. The other furan ring established anion- π interaction with Asp104. The arrangement of these two aromatic groups of the capping moiety, induced by the rim shape of the channel, favoured the coordination of the zinc. It is noteworthy that we designed this cap group in order to discriminate between the isoforms of class I. Indeed, besides the HDAC1 and HDAC2 selectivity driven by the metal binder, we observed that this cap group interacts differently with HDAC1 and HDAC2, leading to a preference towards isoform 2. Moreover, the resolved X-ray structure of HDAC2 (3MAX, pdb ID) presents the protein bound to a N-(2-aminophenyl)benzamide. The comparison of **37** with this N-(2-aminophenyl)benzamide in the catalytic site of HDAC2 revealed a similarity in the binding mode (Figure S11). Both binders present a superimposable appendage at chelating portion that fills the internal cavity. The two small molecules have an

amide group, which occupies equivalent spaces and is involved in the zinc ion coordination. The compound **37** shows a larger cap group than the N-(2-aminophenyl)benzamides. The latter coordinates the zinc ion in bidentate fashion, whereas **37** binds the zinc by only the CO of amide group. In the theoretical model obtained by docking calculations, we observed that the interactions of the cap group with the surface counterpart of HDAC1 prevented the right approaching of metal binder to the zinc, predicting absence or at least scarce biological activity. Compound **38** and **39** presented a different appendage of the metal binder, which caused a different affinity and selectivity for the investigated isoforms. In compound **38**, the reduced dimensions of the metal binder caused fewer interactions with the internal cavity, justifying a lower affinity for the HDAC2. Moreover, the modification of metal binder structure gave rise to a possible binding to the HDAC8 (Figure S12), as suggested by our calculations. This was due to the smaller internal cavity of HDAC8 (see also 3.7) than the remaining class I isoforms, thus the reduced size of the metal binder appendage could favour the maximal interactions with protein residues. The same considerations can be made for the **39** (Figures S13, S14). The **39** presented a metal binder appendage with suitable size for the limited internal cavity of HDAC8. Moreover, we observed for **38** and **39** that their binding to isoforms 8 was also favoured by the shift of Phe152 (see also 3.7), along the hydrophobic 11 Å channel. Respect to **37** and **38**, compound **39** presents a methylene between the chelating agent and the linker. This structural modification does not favour the interactions given by the linker and the cap group with HDAC2. Indeed **39** showed a lower binding affinity with HDAC2, with respect to the other compounds.

Please, insert Figure 6

4.2. Synthesis of **37-39**

Virtual screening driven synthesis of the three derivatives **37-39** relies on the retro-synthetic analysis outlined in Scheme 3(a). We started from the commercially available scaffold A, which was subjected as first to an amidation reaction in order to construct the amido functionality. Then, to insert on the aromatic ring the two amine functions, reduction of NO₂ groups was performed. Finally, to decorate the aromatic scaffold with symmetric appendages, a reductive amination reaction, with the appropriate aldehyde **51-53**, was used. The experimental details of the synthetic procedure are outlined in Scheme 3(b). In particular, taking advantages of the conventional peptide synthesis conditions, we used the carboxylic acids **40** or **41** and the amines **42-44**, in presence of HOBT and DIC as carboxylic group activators, TEA as base and DMF as solvent. Afterward, we first reduced the nitro-group, on the aromatic ring, employing SnCl₂ in ethanol as solvent and heating the mixture of reaction at 80° C for about 30 minutes. Finally, to generate the desired derivatives **37-39**, we subjected the diaminic intermediates **48-50** to a reductive amination with the appropriate aldehydes (**51-53**) using ZnCl₂ as carbonyl group activator in presence of NaCNBH₄. This last reaction required a fine adjustment of the experimental conditions to avoid the by-products formations, mainly constituted by poly-alkylated amines. Systematically variations of the aldehydes amount, the dilutions and the reaction times, allowed to find the optimal conditions for obtaining **37-39** in satisfactory yields (see also Supplementary data).

Please, insert Scheme 3

4.3. Biological Activities

The selectivity of **37-39** was evaluated on HDAC1-4 and HDAC6-8 by experimental assays (Table 2). Compounds **37-39** displayed significant selectivity in the in vitro inhibition tests against the HDAC1-4 and HDAC6-8 (Table 2). As expected, all compounds were not able to inhibit class II HDACs, and showed a selective isoform binding among proteins of class I. As predicted by the docking studies, **37** showed selectivity on HDAC2, thus confirming that the structure of cap group and metal binder is an important determinant for the biological activity towards isoform 2. In particular, the capping moiety allowed to discriminate between HDAC1 and HDAC2. Compared to **37**, compound **38** presented no activity against HDAC2 in agreement to the docking results, due to the less extended interactions given by the pyrrolidine with the internal hydrophobic cavity. As for **37**, **38** did not present activity of isoforms 1 and 3. There was a good activity on HDAC8, probably due to the modified and well tailored metal binder. Concerning compound **39**, the experimental data confirmed the theoretically expected (see Proof of concept) lower/absent selectivity of binding to HDAC2 as theoretically foreseen. Moreover, thank to the cap group an inhibitory activity on HDAC1 was not detected. Compound **39** showed a comparable inhibition of HDAC3 and HDAC8. In summary, **37** and **38** are respectively selective ligands of HDAC2 and of HDAC8, even though at modest potency. The evaluated inhibitory activity on these enzymes is in line with the theoretical findings, confirming the predicted structural observations.

Please insert Table 2

5. Conclusions

In the field of epigenetic cancer therapy, inhibitors of Histone Deacetylases (HDACs) have been gaining a great success. Their potential application in cancers therapy is limited by different side-effects, due to the unselective binding towards either all or at least several HDAC isoforms by the inhibitors. Thus, the further development of HDAC inhibitors is to target selectively individual HDAC isoforms. In the present contribution, the structural elements responsible of the selective binding towards a specific isoform of HDAC have been investigated, and our findings are the initial efforts of a scientific project focusing on the efficacy evaluation of selective binders in cancer therapy.

It should be highlighted that class I and II proteins present a considerable sequence similarity in the catalytic site. The analysis of homology and experimental models revealed the presence of two phenylalanines to shape the channel which accommodates the substrate. Thus, the insertion of an aromatic linker, establishing π - π interactions with these two phenylalanine side chains, could be the starting point to design selective inhibitors of HDACs. As common structural feature of class I enzymes, we found the presence of a CO of a glycine and side chain of a tyrosine pointing inside the 11 Å channel, suggesting the insertion of hydrogen bond donors and acceptors as structural elements to increase the affinity for the isoforms of class I. Class I proteins present an internal pocket at the bottom of the tube-like channel leading to the zinc ion. This internal cavity is formed by the same residues for all class I isoforms, except for HDAC8 presenting a Leu replaced by Tyr. Differences are also observed in the amino acids surrounding the internal cavity, causing diversity in the shape and dimension of this inside pocket across class I isoforms. This internal cavity can be useful to dictate a class I and isoform selectivity, designing a metal binder able to maximize the interactions with this pocket. It is noteworthy that

the shape at the border of the channel leading to the zinc ion, and the relative orientation of these surface pockets respect to the metal and the internal cavity differs in each class I isoforms. Thus, the rational design of capping group able to fit the surface cavities of each isoform, without altering the contacts given by the other structural portions of the ligands can dictate the isoform selectivity. HDAC1 and HDAC2 presents high similarity and identity percentage in the amino acid sequence, but we observed different dimensions in the catalytic pockets of the isoforms 1 and 2. These discrepancies could be ascribable to the differences in the primary sequences of the residues neighbouring the catalytic cavity.

The rationalization of binding mode of APHA derivatives, along with the analysis of all other considered compounds, suggested the structural elements for the specific binding to HDAC4. APHA compounds present a halogenated phenyl ring as cap group, establishing a selective hydrogen bond with the Tyr170 of isoform 4. Moreover, the hydroxamic acid coordinated the zinc ion, but also established hydrogen bonds with the side chains of His158 and His159. Behind the different globular shape, HDAC4, respect to the other proteins of class I and II, presented a different charge distribution in the surface regions bordering the channel which conducts to the zinc ion. Thus, on the capping moiety could be inserted functionality able to electrostatically interact with positively charged regions of HDAC4. Moreover, hydrophobic pockets on the protein surface were found and can be exploited to increase the affinity for HDAC4.

In line with reported studies on selective inhibitors of HDAC6, we observed that the linker length plays a fundamental role in the binding preference towards this isoform. Selective inhibitors of HDAC6 presented a longer linker length than class I selective binders, and our analysis revealed that this structural feature of the ligands favour the extended interactions of cap group with the residues on the surface of the protein. Moreover, combining the right linker length with a large and rigid cap group can also lead towards isoform 6 selectivity.

About HDAC7, the selectivity could be obtained by designing a tailored metal binder able to interact with the unique enlarged binding site of this isoform. Moreover, we observed a peculiar surface hydrophobic pocket at the rim of the channel harbouring the substrate. We suggest that an adapted capping moiety, able to interact with this found cavity, can further lead the binding preference for this protein.

In order to rapidly verify our structural findings, we designed small molecular probes. In particular, we tried to discriminate between HDAC1 and 2, which are very similar isoforms. These designed small molecules were synthesized and tested by *in vitro* inhibitory activity on all considered HDAC isoforms. In particular, we used a weak chelating agent, the carbonyl group, in order to emphasize the contribution to selective binding by the other structural moieties. As expected the small molecules showed a modest potency, but the aim of the presented work is to open a new avenue for a targeted rational design of selective inhibitors towards the different HDAC isoforms. In particular, we found that compound **37** exclusively binds HDAC2, whereas **38** inhibits HDAC8, suggesting that the structural modification of the appendage of the metal binder can lead to isoform selectivity in agreement with theoretical analysis. Moreover, our analysis also suggests the role of cap group to lead to isoforms selectivity. Compound **39** shows similar inhibitory activity on HDAC3 and 8, confirming the theoretical prediction that structural modification of the linker alters the interaction of the cap group with HDAC2. The experimental data confirm as predicted by

theoretical structural observations, and represent a starting point of a research project aimed to obtain more potent a selective compounds. Even though **37-39** are weak binders, we were able to propose new molecular scaffolds, obtainable by few simple synthetic steps, and they could be new useful chemical platforms for the design of selective inhibitors of HDACs. In particular, in the first synthetic step different aromatic platform can be used allowing to differentiate the obtainable compounds and explore the chemical diversity. On this basis, new synthetic, theoretical and experimental studies are in progress to develop more potent inhibitors against a selected HDAC isoform. Moreover, considering that HDACs work in cells as multi-protein complexes, the new studies will also focus on the efficiency to inhibit these protein clusters.

Acknowledgments

Financial support by the University of Salerno and by Ministero dell'Istruzione, dell'Università e della Ricerca (MIUR), PRIN 2009 "Design, conformational and configurational analysis of novel molecular platforms".

References and notes

1. Strahl, B. D.; Allis C. D. *Nature* **2000**, *403*, 41–45.
2. de Ruijter, A. J.; van Gennip, A. H.; Caron, H. N.; Kemp, S.; van Kuilenburg, A. B. *Biochem. J.* **2003**, *370*, 737–749.
3. Michishita, E.; Park, J. Y.; Burneski, J. M.; Barrett, J. C.; Horikawa, I. *Mol. Biol. Cell.* **2005**, *16*, 4623–4635.
4. Bertrand, P. *Eur. J. Med. Chem.* **2010**, *45*, 2095–2116.
5. Witt, O.; Deubzer, H. E.; Milde, T.; Oehme, I. *Cancer Lett.* **2009**, *277*, 8–21.
6. Bolden, J.E.; Peart, M. J.; Johnstone, R. W. *Nat. Rev. Drug Discovery* **2006**, *5*, 769–784.
7. Bieliauskas, A. V.; Pflum, M. K. H. *Chem. Soc. Rev.* **2008**, *37*, 1402–1413.
8. Wang, D. *Curr. Top. Med. Chem.* **2009**, *9*, 241–256.
9. Marks, P. A.; Breslow, R. *Nat. Biotechnol.* **2007**, *25*, 84–90.
10. Furumai, R.; Matsuyama, A.; Kobashi, N.; Lee, K-H.; Nishiyama, M.; Nakajima, H.; Tanaka, A.; Komatsu, Y.; Nishino, N.; Yoshida, M.; Horinouchi, S. *Cancer Res.* **2002**, *62*, 4916–4921. (b) VanderMolen, K. M.; McCulloch, W.; Pearce, C. J.; Oberlies, N.H. *J. Antibiot.* **2011**, *64*, 525–531.
11. Bruserud, O.; Stapnes, C.; Ersvaer, E.; Gjertsen, B. T.; Rynningen, A. *Curr. Pharm. Biotechnol.* **2007**, *8*, 388–400.
12. (a) Bolden, J. E.; Peart, M.J.; Johnstone, R. W. *Nat. Rev. Drug Discov.* **2006**, *5*, 769–784. (b) Thomas, E. A. *Mol. Neurobiol.* **2009**, *40*, 33–45.
13. Bantscheff, M.; Hopf, C.; Savitski, M. M.; Dittmann, A.; Grandi, P.; Michon, A-M.; Schlegl, J.; Abraham, Y.; Becher, I.; Bergamini, G.; Boesche, M.; Dellling, M.; Dümpelfeld, B.; Eberhard, D.; Huthmacher, C.; Mathieson, T.; PoECKel, D.; Reader, V.; Strunk, K.; Sweetman, G.; Kruse, U.; Neubauer, G.; Ramsden, N. G.; Drewes, G. *Nat. Biotechnol.* **2011**, *29*:255–265.
14. (a) Galletti, P.; Quintavalla, A.; Ventrice, C.; Giannini, G.; Cabri, W.; Penco, S.; Gallo, G.; Vincenti, S.; Giacomini, D. *ChemMedChem* **2009**, *4*, 1991–2001. (b) KrennHrubec, K.; Marshall, B. L.; Hedglin, M.; Verdin, E.; Ulrich, S. M. *Bioorg. Med. Chem. Lett.* **2007**, *17*, 2874–2878. (c) Moradei, O. M.; Mallais, T. C.; Frechette, S.; Paquin, I.; Tessier, P. E.; Leit, S. M.; Fournel, M.; Bonfils, C.; Trachy-Bourget, M-C.; Liu, J.; Yan, T. P.; Lu, A-H.; Rahil, J.; Wang, J.; Lefebvre, S.; Li, Z.; Vaisburg, A. F.; Besterman, J. M. *J. Med. Chem.* **2007**, *50*, 5543–5546. (d) Estiu, G.; Greenberg, E.; Harrison, C. B.; Kwiatkowski, N. P.; Mazitschek, R.; Bradner, J. E.; Wiest, O. *J. Med. Chem.* **2008**, *51*, 2898–2906. (e) Schäfer, S.; Saunders, L.; Schlimme, S.; Valkov, V.; Wagner, J. M.; Kratz, F.; Sippl, W.; Verdin, E.; Jung, M. *ChemMedChem* **2009**, *4*, 283–290.
15. (a) Itoh, Y.; Suzuki, T.; Kouketsu, A.; Suzuki, N.; Maeda, S.; Yoshida, M.; Nakagawa, H.; Miyata, N. *J. Med. Chem.* **2007**,

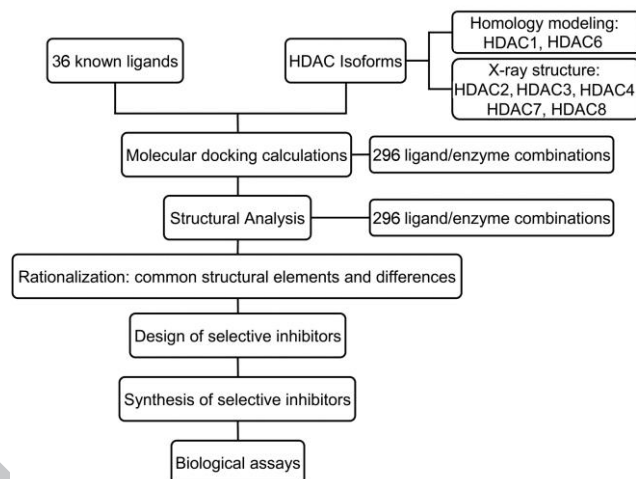
- 50, 5425-5438. (b) Kozikowski, A. P.; Chen, Y.; Gaysin, A.; Chen, B.; D'Annibale, M. A.; Suto, C. M.; Langley, B. C. **2007**, *J. Med. Chem.* **50**, 3054-3061. (c) Mai, A.; Massa, S.; Pezzi, R.; Simeoni, S.; Rotili, D.; Nebbioso, A.; Scognamiglio, A.; Altucci, L.; Loidl, P.; Brosch, G. *J. Med. Chem.* **2005**, **48**, 3344-3353. (d) Siliphaivanh, P.; Harrington, P.; Witter, D. J.; Otte, K.; Tempest, P.; Kattar, S.; Kral, A. M.; Fleming, J. C.; Deshmukh, S. V.; Harsch, A.; Secrist, P. J.; Miller, T. A. *Bioorg. Med. Chem. Lett.* **2007**, **17**, 4619-4624.
16. Altschul, S. F.; Gish, W.; Miller, W.; Myers, E. W.; Lipman, D. J. *J. Mol. Biol.* **1990**, **215**, 403-410.
17. Henikoff, S.; Henikoff, J. G. *Proc. Natl. Acad. Sci. USA* **1992**, **89**, 10915-10919.
18. Pettersen, E. F.; Goddard, T. D.; Huang, C. C.; Couch, G. S.; Greenblatt, D. M.; Meng, E. C.; Ferrin, T. E. *J. Comput. Chem.* **2004**, **25**, 1605-1612.
19. Wang, D. F.; Helquist, P.; Wiech, N. L.; Wiest, O. *J. Med. Chem.* **2005**, **48**, 6936-6947.
20. Ayer, D. E. *Trends Cell Biol.* **1999**, **9**, 193-198.
21. Bressi, J. C.; Jennings, A. J.; Skene, R.; Wu, Y.; Melkus, R.; De Jong, R.; O'Connell, S.; Grimshaw, C. E.; Navre, M.; Gangloff, A. R. *Bioorg. Med. Chem. Lett.* **2010**, **20**, 3142-3145.
22. Bottomley, M. J.; Lo Surdo, P.; Di Giovine, P.; Cirillo, A.; Scarpelli, R.; Ferrigno, F.; Jones, P.; Neddermann, P.; De Francesco, R.; Steinkuhler, C.; Gallinari, P.; Carfi, A. *J. Biol. Chem.* **2008**, **283**, 26694-26704.
23. Zou, H.; Wu, Y.; Navre, M.; Sang, B. C. *Biochem. Biophys. Res. Commun.* **2006**, **341**, 45-50.
24. Butler, K. V.; Kalin, J.; Brochier, C.; Vistoli, G.; Langley, B.; Kozikowski, A. P. *J. Am. Chem. Soc.* **2010**, **132**, 10842-10846.
25. Fiser, A.; Sali, A. *Meth. Enzymol.* **2003**, **374**, 461-91.
26. Kaminski, G. A.; Friesner, R. A.; Tirado-Rives, J.; Jorgensen, W. L. *J. Phys. Chem. B* **2001**, **105**, 6474-6487.
27. MacroModel, version 8.5, Schrödinger LLC, New York, NY, **2003**
28. Laskowski, R. A.; MacArthur, M. W.; Moss, D. S.; Thornton, J. M. *J. App. Cryst.* **1993**, **26**, 283-291.
29. Zhao, Y.; Schultz, N. E.; Truhlar, D. G. *J. Chem. Phys.* **2005**, **123**, 161103-1-4.
30. Breneman, C. M.; Wiberg, K. B. *J. Comput. Chem.* **1990**, **11**, 361-373.
31. Gaussian 03, Revision E.01, Frisch, M. J.; Trucks, G. W.; Schlegel, H. B.; Scuseria, G. E.; Robb, M. A.; Cheeseman, J. R.; Montgomery, J. A., Jr.; Vreven, T.; Kudin, K. N.; Burant, J. C.; Millam, J. M.; Iyengar, S. S.; Tomasi, J.; Barone, V.; Mennucci, B.; Cossi, M.; Scalmani, G.; Rega, N.; Petersson, G. A.; Nakatsuji, H.; Hada, M.; Ehara, M.; Toyota, K.; Fukuda, R.; Hasegawa, J.; Ishida, M.; Nakajima, T.; Honda, Y.; Kitao, O.; Nakai, H.; Klene, M.; Li, X.; Knox, J. E.; Hratchian, H. P.; Cross, J. B.; Adamo, C.; Jaramillo, J.; Gomperts, R.; Stratmann, R. E.; Yazyev, O.; Austin, A. J.; Cammi, R.; Pomelli, C.; Ochterski, J. W.; Ayala, P. Y.; Morokuma, K.; Voth, G. A.; Salvador, P.; Dannenberg, J. J.; Zakrzewski, V. G.; Dapprich, S.; Daniels, A. D.; Strain, M. C.; Farkas, O.; Malick, D. K.; Rabuck, A. D.; Raghavachari, K.; Foresman, J. B.; Ortiz, J. V.; Cui, Q.; Baboul, A. G.; Clifford, S.; Cioslowski, J.; Stefanov, B. B.; Liu, G.; Liashenko, A.; Piskorz, P.; Komaromi, I.; Martin, R. L.; Fox, D. J.; Keith, T.; Al-Laham, M. A.; Peng, C. Y.; Nanayakkara, A.; Challacombe, M.; Gill, P. M. W.; Johnson, B.; Chen, W.; Wong, M. W.; Gonzalez, C.; Pople, J. A. (2004) Gaussian, Inc., Wallingford CT.
32. Halgren, T. A. *J. Comput. Chem.* **1996**, **17**, 616-641.
33. Still, W. C.; Tempczyk, A.; Hawley, R. C.; Hendrickson, T. *J. Am. Chem. Soc.* **1990**, **112**, 6127-6129.
34. Morris, G. M.; Goodsell, D. S.; Halliday, R. S.; Huey, R.; Hart, W. E.; Belew, R. K.; Olson, A. J. *J. Comp. Chem.* **1998**, **19**, 1639-1662.
35. Maulucci, N.; Chini, M. G.; Di Micco, S.; Izzo, I.; Cafaro, E.; Russo, A.; Gallinari, P.; Paolini, C.; Nardi, M. C.; Casapullo, A.; Riccio, R.; Bifulco, G.; De Riccardis, F. *J. Am. Chem. Soc.* **2007**, **129**, 3007-3012.
36. (a) Di Micco, S.; Terracciano, S.; Bruno, I.; Rodriguez, M.; Riccio, R.; Taddei, M.; Bifulco, G. *Bioorg. Med. Chem.* **2008**, **16**, 8635-8642. (b) Grolla, A. A.; Podesta, V.; Chini, M. G.; Di Micco, S.; Vallario, A.; Genazzani, A. A.; Canonico, P. L.; Bifulco, G.; Tron, G. C.; Sorba, G.; Pirali, T. *J. Med. Chem.* **2009**, **52**, 2776-2785. (c) Pirali, T.; Faccio, V.; Mossetti, R.; Grolla, A. A.; Di Micco, S.; Bifulco, G.; Genazzani, A. A.; Tron, G. C. *Mol. Diversity* **2010**, **14**, 109-121. (d) Terracciano, S.; Di Micco, S.; Bifulco, G.; Gallinari, P.; Riccio, R.; Bruno, I. *Bioorg. Med. Chem.* **2010**, **18**, 3252-3260. (e) Terracciano, S.; Chini, M. G.; Bifulco, G.; D'Amico, E.; Marzocco, S.; Riccio, R.; Bruno, I. *Tetrahedron* **2010**, **66**, 2520-2528.
37. Watson, P. J.; Fairall, L.; Santos, G. M.; Schwabe, J. W. R. *Nature* **2012**, **481**, 335-340.
38. Schuetz, A.; Min, J.; Allali-Hassani, A.; Schapira, M.; Shuen, M.; Loppnau, P.; Mazitschek, R.; Kwiatkowski, N. P.; Lewis, T. A.; Maglathin, R. L.; McLean, T. H.; Bochkarev, A.; Plotnikov, A. N.; Vedadi, M.; Arrowsmith, C. H. *J. Biol. Chem.* **2008**, **283**, 11355-11363.
39. Dowling, D. P.; Gantt, S. L.; Gattis, S. G.; Fierke, C. A.; Christianson, D. W. *Biochemistry* **2008**, **47**, 13554-13563.
40. Somoza, J. R.; Skene, R. J.; Katz, B. A.; Mol, C.; Ho, J. D.; Jennings, A. J.; Luong, C.; Arvai, A.; Buggy, J. J.; Chi, E.; Tang, J.; Sang, B.-C.; Verner, E.; Wynands, R.; Leahy, E. M.; Dougan, D. R.; Snell, G.; Navre, M.; Knuth, M. W.; Swanson, R. V.; McRee, D. E.; Tari, L. W. *Structure* **2004**, **12**, 1325-1334.
41. Stote, R. H.; Karplus, M. *Proteins* **1995**, **23**, 12-31.
42. Finnin, M. S.; Donigian, J. R.; Cohen, A.; Richon, V. M.; Rifkind, R. A.; Marks, P. A.; Pavletich, N. P. *Nature* **1999**, **401**, 188-193.
43. Wang, D. F.; Wiest, O.; Helquist, P.; Lan-Hargest, H. Y.; Wiech, N. L. *J. Med. Chem.* **2004**, **47**, 3409-3417.
44. (a) Methot, J. L.; Hamblett, C. L.; Mampreian, D. M.; Jung, J.; Harsch, A.; Szweczek, A. A.; Dahlberg, W. K.; Middleton, R. E.; Hughes, B.; Fleming, J. C.; Wang, H.; Kral, A. M.; Ozerova, N.; Cruz, J. C.; Haines, B.; Chenard, M.; Kenific, C. M.; Secrist, J. P.; Miller, T. A. *Bioorg. Med. Chem. Lett.* **2008**, **18**, 6104-6109. (b) Hamblett, C. L.; Methot, J. L.; Mampreian, D. M.; Sloman, D. L.; Stanton, M. G.; Kral, A. M.; Fleming, J. C.; Cruz, J. C.; Chenard, M.; Ozerova, N.; Hitz, A. M.; Wang, H.; Deshmukh, S. V.; Nazef, N.; Harsch, A.; Hughes, B.; Dahlberg, W. K.; Szweczek, A. A.; Middleton, R. E.; Mosley, R. T.; Secrist, J. P.; Miller, T. A. *Bioorg. Med. Chem. Lett.* **2007**, **17**, 5300-5309.
45. Saito, A.; Yamashita, T.; Mariko, Y.; Nosaka, Y.; Tsuchiya, K.; Ando, T.; Suzuki, T.; Tsuruo, T.; Nakanishi, O. *Proc. Natl. Acad. Sci. USA* **1999**, **96**, 4592-4597.
46. Byrd, J. C.; Marcucci, G.; Parthun, M. R.; Xiao, J. J.; Klisovic, R. B.; Moran, M.; Lin, T. S.; Liu, S.; Sklenar, A. R.; Davis, M. E.; Lucas, D. M.; Fischer, B.; Shank, R.; Tejaswi, S. L.; Binkley, P.; Wright, J.; Chan, K. K.; Grever, M. R. *Blood* **2005**, **105**, 959-967.
47. Singh, S. B.; Zink, D. L.; Liesch, J. M.; Mosley, R. T.; Dombrowski, A. W.; Bills, G. F.; Darkin-Rattray, S. J.; Schmatz, D. M.; Goetz, M. A. *J. Org. Chem.* **2002**, **67**, 815-825.
48. Atadja, P.; Gao, L.; Kwon, P.; Trogani, N.; Walker, H.; Hsu, M.; Yeleswarapu, L.; Chandramouli, N.; Perez, L.; Versace, R.; Wu, A.; Sambucetti, L.; Lassota, P.; Cohen, D.; Bair, K.; Wood, A.; Remiszewski, S. *Cancer Res.* **2004**, **64**, 689-695.
49. Witter, D. J.; Harrington, P.; Wilson, K. J.; Chenard, M.; Fleming, J. C.; Haines, B.; Kral, A. M.; Secrist, J. P.; Miller, T. A. *Med. Chem. Lett.* **2008**, **18**, 726-731.
50. Hu, E.; Dul, E.; Sung, C.-M.; Chen, Z.; Kirkpatrick, R.; Zhang, G.-F.; Johanson, K.; Liu, R.; Lago, A.; Hofmann, G.; Macarron, R.; De Los Frailes, M.; Perez, P.; Krawiec, J.; Winkler, J.; Jaye, M. *J. Pharmacol. Exp. Ther.* **2003**, **307**, 720-728.
51. (a) Liang, J.; Edelsbrunner, H.; Woodward, C. *Protein Sci.* **1998**, **7**, 1884-1897. (b) Liang, J.; Edelsbrunner, H.; Fu, P.; Sudhakar, P. V.; Subramaniam, S. *Proteins* **1998**, **33**, 18-29. (c) Liang, J.; Edelsbrunner, H.; Fu, P.; Sudhakar, P. V.; Subramaniam, S. *Proteins* **1998**, **33**, 1-17.
52. Somoza, J. R.; Skene, R. J.; Katz, B. A.; Mol, C.; Ho, J. D.; Jennings, A. J.; Luong, C.; Arvai, A.; Buggy, J. J.; Chi, E.; Tang, J.; Sang, B.-C.; Verner, E.; Wynands, R.; Leahy, E. M.; Dougan, D. R.; Snell, G.; Navre, M.; Knuth, M. W.; Swanson, R. V.; McRee, D. E.; Tari, L. W. *Structure* **2004**, **12**, 1325-1334.

53. Balasubramanian, S.; Ramos, J.; Luo, W.; Sirisawad, M.; Verner, E.; Buggy, J. J. *Leukemia* **2008**, *22*, 1026-1034.
54. Mai, A.; Jelicic, K.; Rotili, D.; Di Noia, A.; Alfani, E.; Valente, S.; Altucci, L.; Nebbioso, A.; Massa, S.; Galanello, R.; Brosch, G.; Migliaccio, A. R.; Migliaccio, G. *Mol. Pharmacol.* **2007**, *72*, 1111-1123.
55. Haggarty, S. J.; Koeller, K. M.; Wong, J. C.; Butcher, R. A.; Schreiber, S. L. *Chem. Biol.* **2003**, *10*: 383-396.
56. Suzuki, T.; Kouketsu, A.; Itoh, Y.; Hisakawa, S.; Maeda, S.; Yoshida, M.; Nakagawa, H.; Miyata, N. *J. Med. Chem.* **2006**, *49*, 4809-4812.
57. Butler, K. V.; Kalin, J.; Brochier, C.; Vistoli, G.; Langley, B.; Kozikowski, A. P. *J. Am. Chem. Soc.* **2010**, *132*, 10842-10846.

	isoform	Expression in tumor tissues
	HDAC1	gastric, pancreatic, colorectal, prostate cancer; hepatocellular carcinoma
Class I	HDAC2	colorectal cancer: upregulated in polyps; cervical carcinoma; gastric and prostate cancer: increased expression associated with advanced stage
	HDAC3	gastric, prostate, colorectal cancers
	HDAC8	childhood neuroblastoma
Class IIA	HDAC4	breast cancer
	HDAC7	colorectal cancer
Class IIA	HDAC6	oral squamous cell cancer; breast cancer

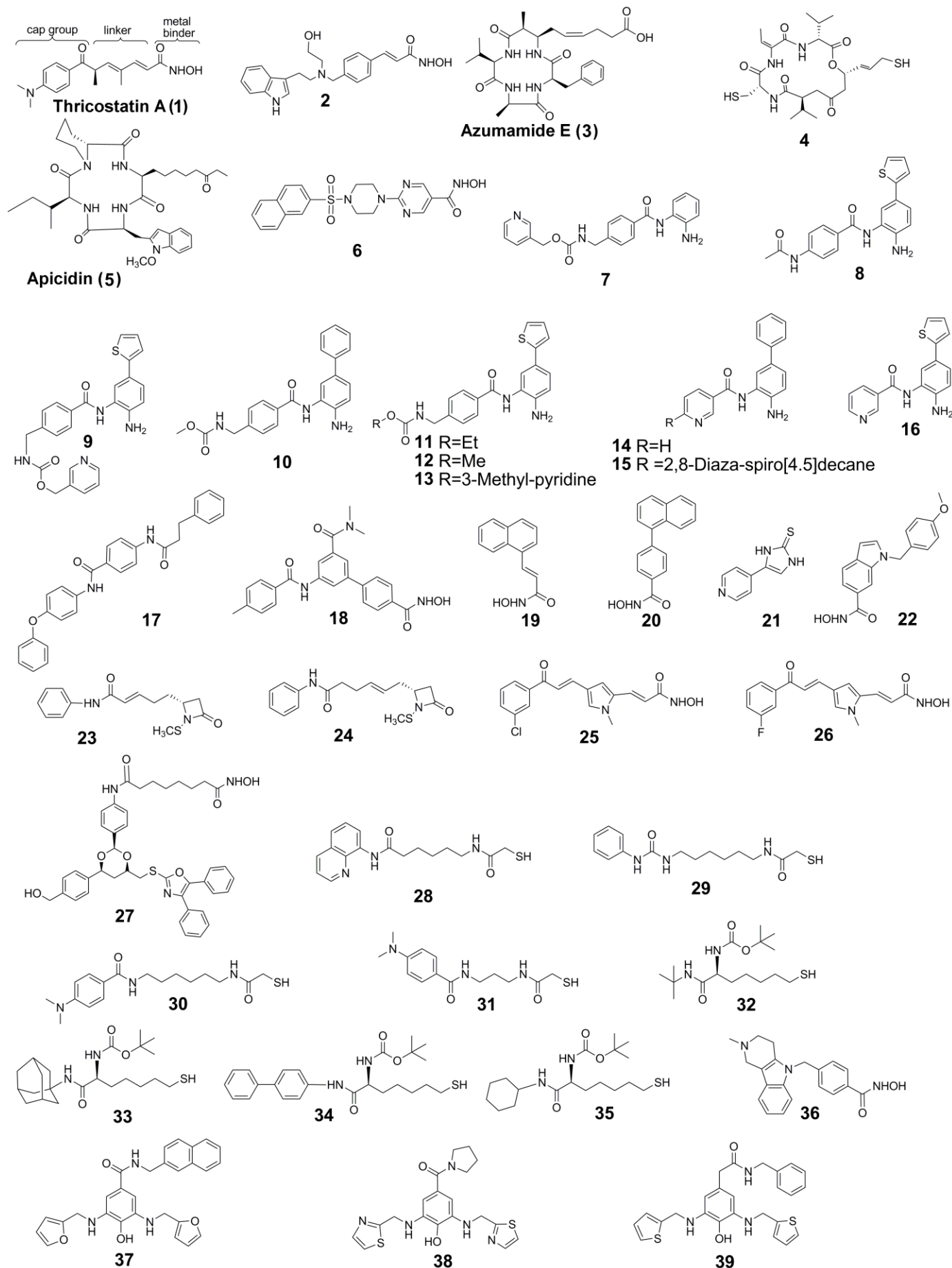
Supplementary Material

Supplementary material associated with this article can be found, in the online version.



Scheme 1. Work-flow of the different stages involved in the structural characterization, design and synthesis of new selective HDAC inhibitors.

Table 1. Expression of HDACs in tumor tissues (see also reference 5).



Scheme 2. Molecular structures of compounds **1-39**. **1** and **2**, pan inhibitors. **3-7**, class I selective inhibitors. **8-17**, HDAC1,2 selective inhibitors. **18-24**, HDAC8 selective inhibitors. **25** and **26**, HDAC4 selective inhibitors. **27-36**, HDAC6 selective inhibitors. **37-39**, designed compounds (see Proof of concept). **4** is the *in vivo* reduced active compound of FK228.

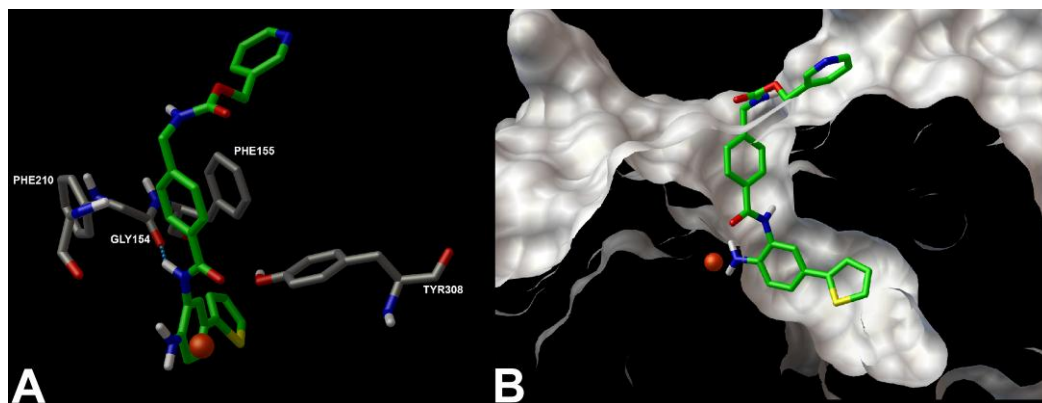


Figure 1. Three-dimensional model of the interactions between **8** and HDAC2. The protein (a) and **8** are represented by tube and their atoms are coloured by atom type: C, gray; polar H, white; N, dark blue; O, red. For **8**, carbon and bonds are depicted in green. The zinc ion is represented in orange cpk. The figure highlights the hydrogen bond (dashed cyan line) between the NH of the amide functionality and the carbonyl of the Gly154. b) The protein is represented by molecular surface. The figure shows the coordination of zinc ion (represented in red cpk) and the accommodation of metal binder appendage in the internal cavity.

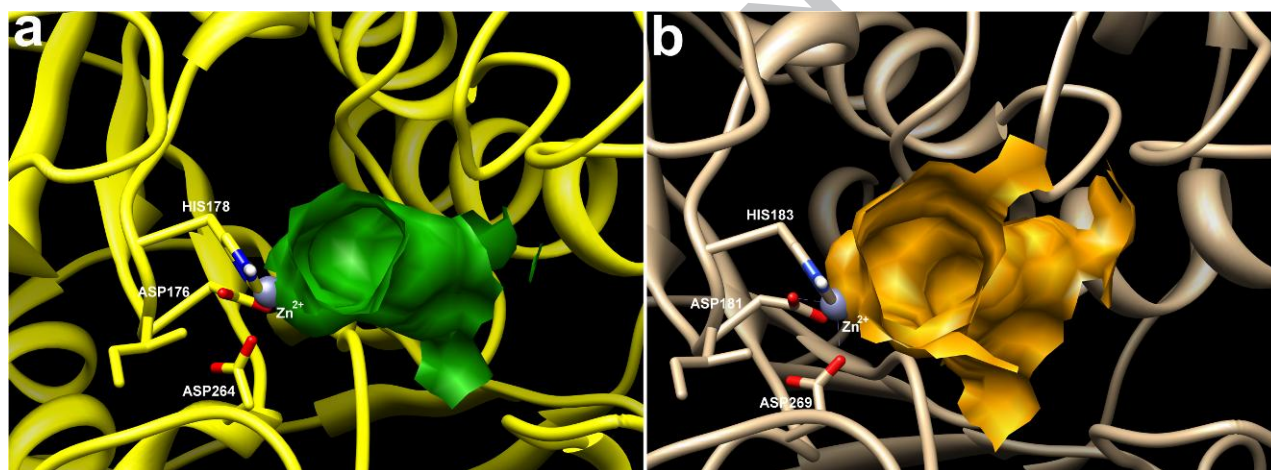


Figure 2. View of the top of the ≈ 11 Å channel. The HDAC1 (a) and HDAC2 (b) are represented by ribbons and their catalytic site by molecular surface coloured in green and orange, respectively. The zinc ion is depicted by light blue cpk. The chelating amino acids are shown by tube, coloured by atom type: polar H, white; O, red. The C atoms of the amino acids are coloured as for the ribbons: yellow (a) and tan (b). The figure highlights the difference in shape and dimensions of the tube like channel, leading to the zinc ion.

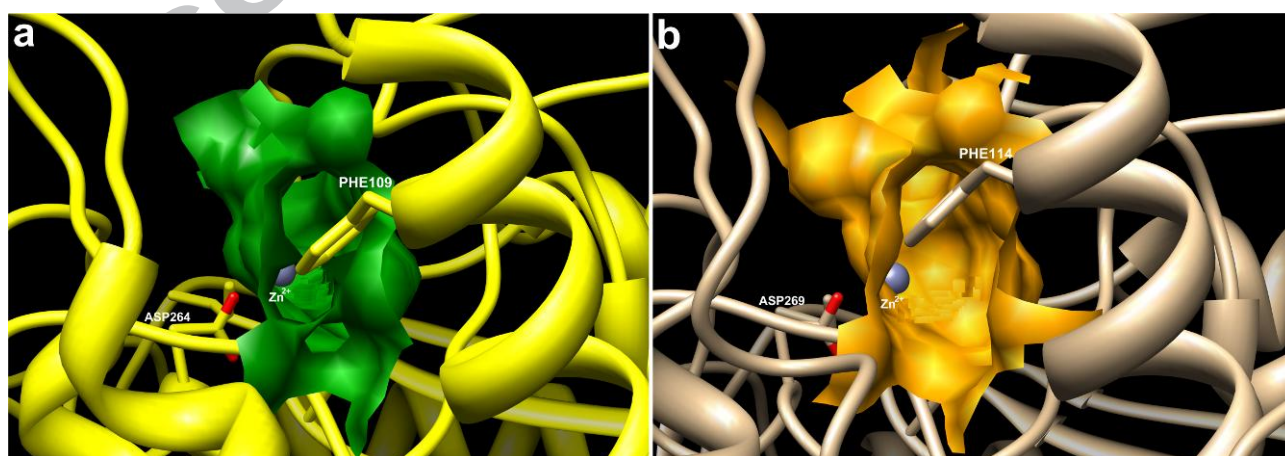


Figure 3. View of the bottom of the side channel. The HDAC1 (a) and HDAC2 (b) are represented by ribbons and their catalytic site by molecular surface coloured in green and orange, respectively. The zinc ion is depicted by light blue cpk. The amino acids are shown by tube, coloured by atom type: polar H, white; O, red. The C atoms of the amino acids are coloured as for the ribbons: yellow (a) and tan (b). The figure highlights the difference in shape and dimensions of the internal channel, near to the catalytic site of the enzymes.

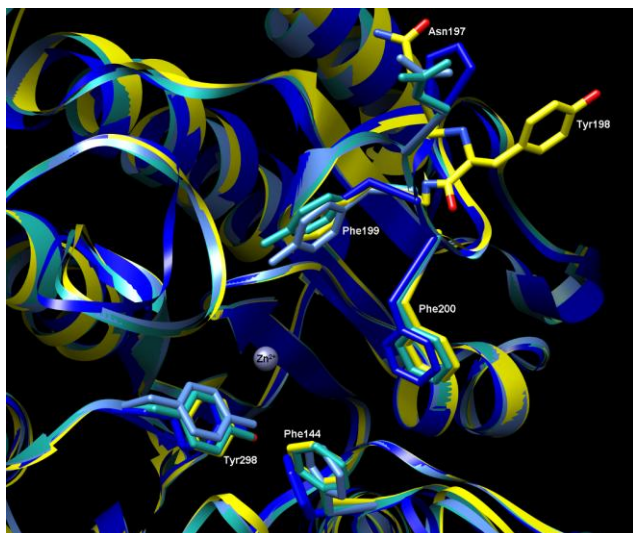


Figure 4. Superimposition of HDAC1 (light blue), HDAC2 (cyan), HDAC3 (yellow) and HDAC8 (blue). The enzymes are represented by ribbons and tube. The zinc ion is depicted as purple cpk. The figure highlights the presence of an extra tyrosine (TYR198) in HDAC3 compared to the other class I proteins.

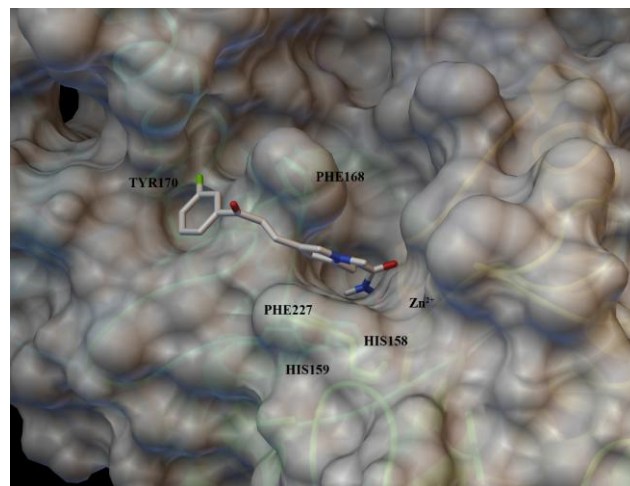


Figure 5. Three-dimensional model of the interactions between **26** and HDAC4. The protein is represented by ribbon and the zinc ion is depicted in dark orange cpk. The side chains of His158, His159 and Tyr170 (light green), and **26** (white) are shown by tube. The atoms are coloured as: polar H, white; N, dark blue; O, red. The yellow dashed lines indicate hydrogen bonds.

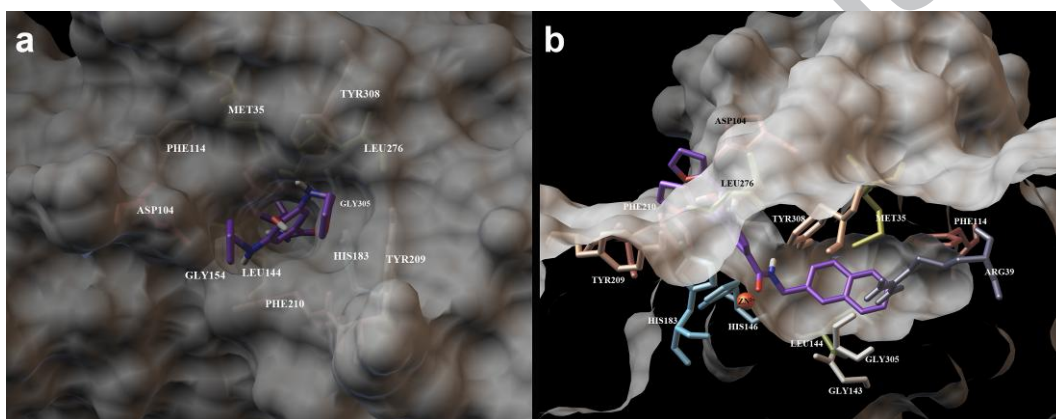
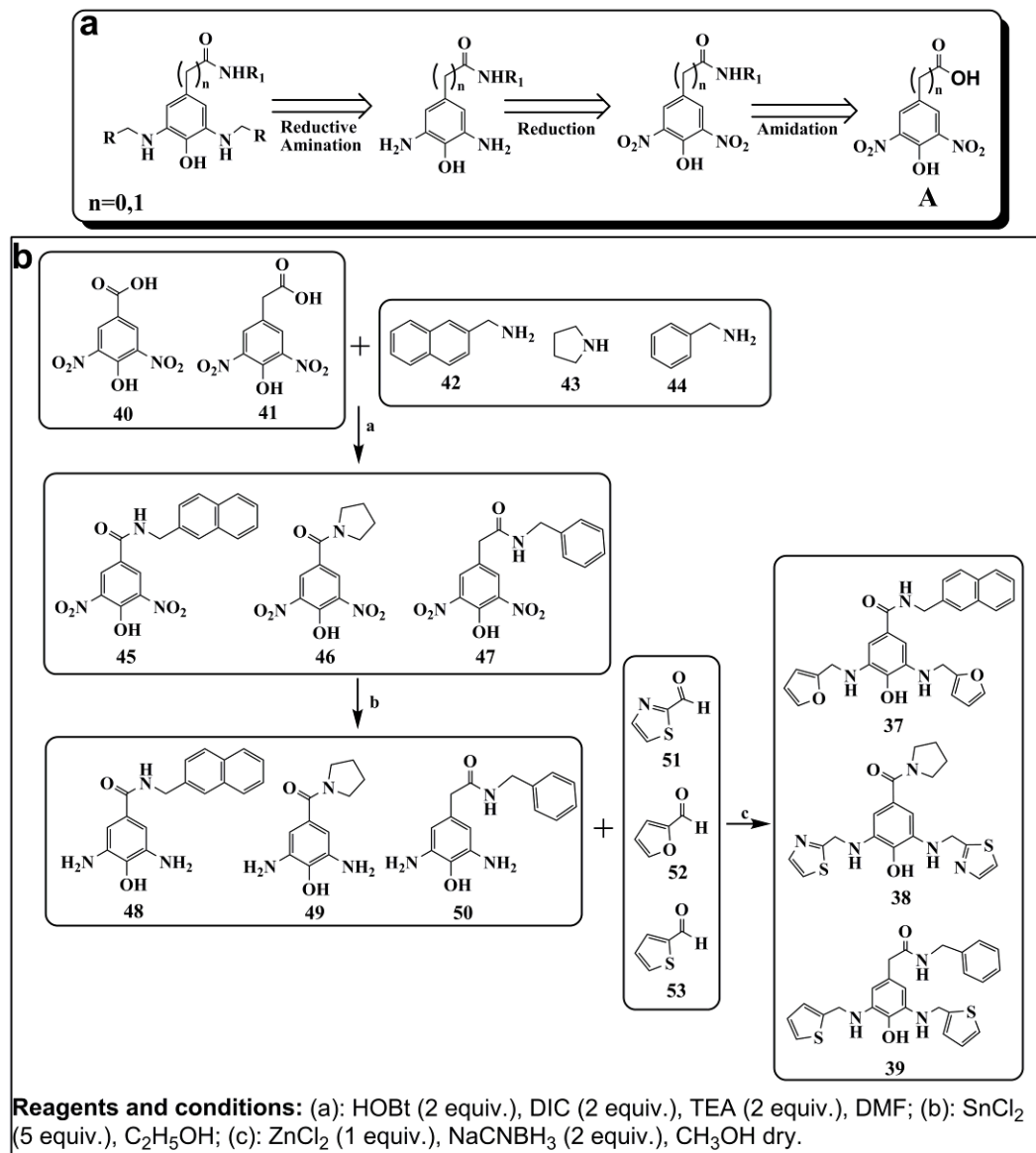


Figure 6. Three-dimensional model of the interactions between **37** and HDAC2. The protein is represented by molecular surface and the zinc ion is depicted in dark orange cpk. The side chains of amino acids are represented by tube, and coloured as: gly, white; asp, red; phe, brown; his, light blue; leu, green; cys, yellow; arg, dark blue; met, olive. The **37** is depicted in purple tube and the atoms are coloured as: C, purple; polar H, white; N, dark blue; O, red.



Scheme 3. a) Retro-synthetic approach for the synthesis of derivatives 37-39. b) Synthetic approach for the synthesis of compounds 37-39.

Table 2. Percentage of residual HDAC activity for compounds 37-39 and TSA as reference, obtained at a concentration of 3.3×10^{-5} M.^{a,b}

compound	HDAC subtype							
	1	2	3	4	6	7	8	
37	-	69.38	-	-	-	-	-	
38	-	-	-	-	-	-	53.58	
39	-	-	53.20	-	-	-	60.65	
TSA	0.02	0.07	0.95	59.23	5.12	35.37	5.72	

^aEmpty cells indicate percentage of activity > 75 %.

^bThe values are calculated at 95% confidence intervals.